PROBABILISTIC CALIBRATION OF AVALANCHE BLOCK MODELS

Peter Gauer[1,2]*, Zenon Medina-Cetina[2], Karstein Lied[1], and Krister Kristensen[1]

[1]Norwegian Geotechnical Institute, Postboks 3930 Ullevål Stadion, 0806 Oslo, Norway
[2]International Centre for Geohazards, c/o Norwegian Geotechnical Institute, Oslo, Norway

ABSTRACT. The Norwegian Geotechnical Institute (NGI) has been operating the full-scale avalanche test-site Ryggfonn in western Norway for more than 25 years. During those years, measurements from about three dozen dry-snow avalanches have provided information on front velocities and runout distances.
Some of those measurements were used to calibrate a simple avalanche model following a well-defined probabilistic method. Traditionally, model parameters of those kinds of models were evaluated from runout analysis disregarding any dynamics. The set of roughly 20 observed avalanches from one single path including, estimations of the front velocities at three points in the lower third of the track provided a unique opportunity for introducing uncertainty quantification methods for evaluating the performance of similar kind of competing models.
We present the model calibration and results from the model performance testing.

Keywords: probabilistic avalanche modeling, Bayesian modeling, calibration, prior knowledge, stochastic framework

1 INTRODUCTION

In avalanche prone areas, hazard and risk assessment for landuse planning involves the estimation of the runout of potential avalanches. Methods for determination of the runout may be grouped into two groups: 1) based on statistical methods like the $\alpha - \beta$ model (Lied and Bakkehøi, 1980), or 2) based on numerical avalanche models like the PCM-model (Perla et al., 1980) or Voellmy-Salm type models (Salm et al., 1990). It is certainly true that there are more sophisticated models as the mentioned ones, but these simple models are sufficient for the purpose of the present paper, and many of the more sophisticated models are based on similar rheological approaches.

Whereas the determination of the runout distance using statistical runout models may be sufficient for a hazard assessment, a risk assessment requires also an evaluation of the consequences. In the case of landuse planning, this involves the estimate on destructive forces due to the avalanche, and requires velocity and density estimates of the avalanche. To that end, numerical models are often times the tool of choice. However, numerical models need a calibration of the their parameters, and if they are used in a probabilistic approach, probability distribution functions of parameters are needed. In the cases of the PCM-model and Voellmy-Salm type models, two parameters need to be determined. Traditionally, these parameters were estimated by back calculation of observed runout distance (e.g. Buser and Frutiger, 1980; Bozhinskiy, 2008). Using only the runout distance provides only one constraint for two parameters. That is insufficient to obtain a unique parameter set. Only in few cases, information on velocity observations were used, for example Ancey and Meunier (2004), who based their analysis on 15 documented events reported in the literature. The avalanches however originated from different paths.

In the following, we present a model calibration based on on the Bayesian paradigm using infirmation from front velocity measurements and observed runout distances from a single path. In this way, it is possible to obtain probability distribution functions that may be used in probabilistic avalanche modeling.

*Corresponding author's address:
Peter Gauer
Norwegian Geotechnical Institute,
P.O. Box 3930 Ullevål Stadion, NO–0806 Oslo, Norway
Tel: ++47 22 02 31 29; Fax: ++47 22 23 04 48; E-mail: pg@ngi.no

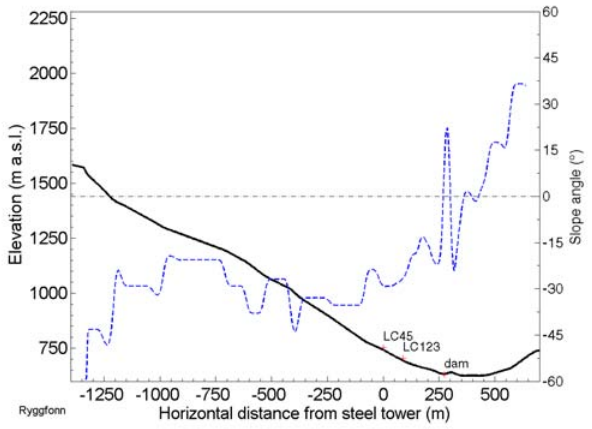

Figure 1: Profile of the main avalanche track; the locations of the steel pylon (LC45), the concrete wedge (LC123), and of the foot of the dam are marked with crosses.

2 RYGGFONN TEST-SITE

The Norwegian Geotechnical Institute (NGI) has been operating the full-scale avalanche test-site Ryggfonn, Western Norway, for more than 25 years. The main track starts at rim of a north facing bowl and has a total drop height of about 900 m. The path itself is slightly canalized. The horizontal runout distance ranges typically between 1500 and 1850 m. Figure 1 shows a profile of the path. One particular characteristic of this test-site is a 16 m high catching dam in the runout zone. A more detailed description of the test-site and its instrumentation can be found, for example, in (Gauer et al., 2007a, 2008; Faug et al., 2008).

Typical avalanche sizes range between 10^4 m^3 and 10^5 m^3 snow, and maximum front velocities are up to 60 m s^{-1}. Observations from this site include dry and wet snow avalanches.

3 DATA ANALYSIS

From a total of approximately 70 to 80 observed avalanches, data of 22 dry snow avalanches following the main track, were available for this study. For all except of one, there is velocity and runout distance information in the lower third of the track. For the 19831031 event, only the runout is known.

Table 1 summarizes the velocity and runout data. The estimated speeds are based on measurements, (i.e. the timing of the front arrival at various sensors) and/or timing of observations (e.g. video analysis) (Gauer and Kristensen, 2005; Norem, 1995). Relating a mean velocity to the midpoint between pairs of the sensors may introduce a slight error with respect to the real velocity at this location. This correction however is not always possible or may introduce an even higher uncertainty and therefore no correction was preformed here.

Figure 2 plots the fraction of observed runout distances (i.e. the ratio between number of observations per bin to the total number of observations). It also shows the corresponding cumulative frequency. The median coincide with the location of the dam and a major number of avalanches just stop around the dam. If the dam stopped those avalanches or if they had stopped more or less independently is an open question, although, it is not of concern for this study. However, there is also an approximately 50% chance that one of the analyzed avalanches overtopped the dam. At this point it is worthwhile to mention that the data set is biased in this sense that it contains more data from medium to large size avalanches. This is due to fact that many observation origin from artificially re-

Table 1: Analyzed avalanches with respect to the runout[a]

#	Date yyyymmdd	U_{LC} (m s^{-1})	U_{CD} (m s^{-1})	U_b (m s^{-1})	l_r (m)
1	19750225	50	35	22	200
2	19831031	NaN	NaN	NaN	0
3	19840302	30	22	0	-20
4	19850213	34	26	17	70
5	19870128	48	44	40	225
6	19880315	20	1	–	-120
7	19880411	38	33	27	45
8	19890217	22	1	–	-100
9	19890403	22	13	–	-30
10	19920311	0	–	–	-326
11	19930327	43	38	33	150
12	19940318	31	28	25	80
13	19950303	35	32	28	80
14	19970208	45	43	40	195
15	19970417	34	3	0	0
16	19990122	20	12	3	0
17	20000217	50	38	30	333
18	20030406	15	0	–	-150
19	20040224	32	28	22	111
20	20040228	38	22	15	-10
21	20050416	33	6	–	-50
22	20070322	35	15	0	0

[a] U_{LC} is the measured mean velocity of the front between the steel tower and the concrete wedge and related to the midpoint between both locations; U_{CD} is the velocity related to the midpoint between the concrete wedge and the upstream base of the dam; U_b the front speed at the upstream base of the dam; and l_r is the runout along the track measured relative to the crown of the dam (offset $s_{dam} \approx 1940$ m). Estimated error ranges are: $\Delta U/U \approx \pm 0.1$; $\Delta l_r/l_r \approx \pm 0.1$;.

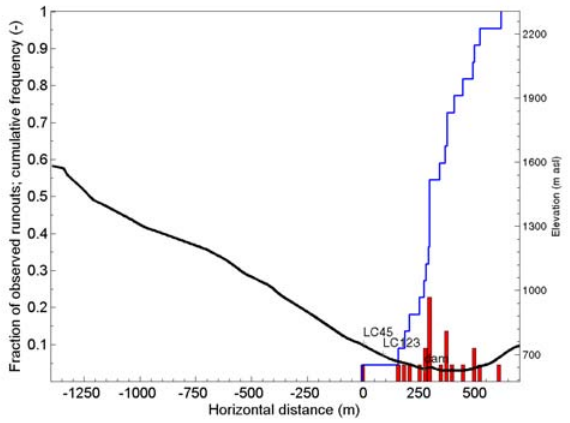

Figure 2: Fraction of observed runout distances (25 m bins) and corresponding cumulative frequency; the locations of the steel pylon (LC45) the concrete wedge (LC123), and of the upstream base of the dam are marked with crosses.

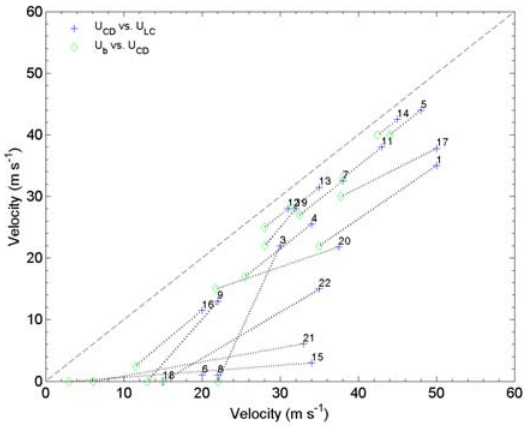

Figure 4: Scatter diagram U_{CD} vs. U_{LC}, and U_b vs. U_{CD}. Numbers mark the respective event. The dotted lines connect measurements form the same event. The dashed line is thought as a guidance and indicates a one to one correlation.

leased avalanche, and smaller natural releases which may have stopped in the upper part of the track especially in the upper bowl were not observed or documented.

Figure 3 shows the cumulative frequency of the velocities U_{LC}, U_{CD}, and U_b (see explanation in Table 1). The scatter diagram in Figure 4 suggest that the velocities are partly correlated. This is not that of a surprise, but it is of importance in the following Bayesian calibration. Figure 5 plots the mean retarding acceleration, $a_{ret_{LD}}$, for the stretch between the midpoint of the steel pylon and the concrete wedge (referred as LC), and the base of the dam versus the mean front speed between those points ($U_{av} = (U_{LC} + U_b)/2$), for those avalanches that at least reached the dam. The retarding acceleration seems to be independent of mean velocity (there is no significant correlation) and rather constant with a mean of about $-4.6 \pm 0.8\,\mathrm{m\,s^{-2}}$. This value is slightly higher than the one given in (Faug et al., 2008), where only those avalanches which overtopped the dam were investigated. Nonetheless, the values are in agreement with recent pulsed doppler measurements (Gauer et al., 2007b).

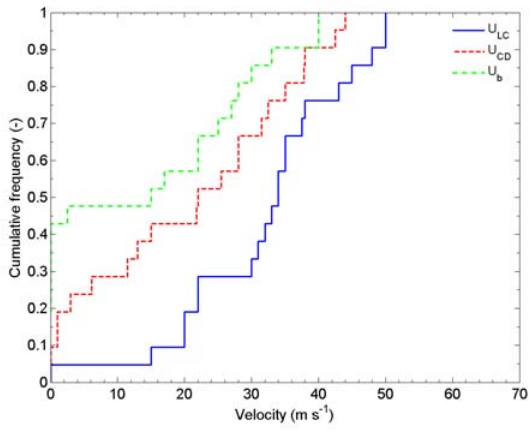

Figure 3: Cumulative frequency of the observed velocities U_{LC}, U_{CD}, and U_b.

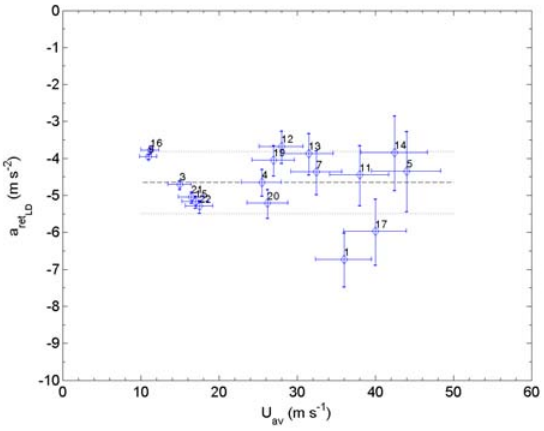

Figure 5: Retarding acceleration, $a_{ret_{LD}}$, between LC and the base of the dam vs. the averaged speed $U_{av} = (U_{LC} + U_b)/2$. The dashed line shows the mean and the dotted ones plot $\pm$ one standard deviation. Numbers mark the respective event.

4 AVALANCHE BLOCK MODELS

In the following we present the results of a Bayesian calibration of a simple block model.

$$\frac{dU^2}{2\,ds} = g\sin\phi + a_{ret}\,, \tag{1}$$

where U is the velocity of the mass block, s the travel distance along the track, g is the acceleration due to gravity and ϕ the local slope angle. For the retarding acceleration, a_{ret}, the following approaches were investigated:

- Coulomb-type, including centrifugal forces

$$a_{ret} = -a_0\ \max(0, g\cos\phi + \kappa U^2)\,, \tag{2$_1$}$$

  where a_0 is the friction factor and κ the curvature of the track;

- PCM-type (Perla et al., 1980);

$$a_{ret} = -a_0\ \max(0, g\cos\phi + \kappa U^2) - a_2 U^2\,, \tag{2$_2$}$$

  where a_2 is a parameter;

- constant deceleration

$$a_{ret} = -a_3\,, \tag{2$_3$}$$

  where a_3 is a constant;

The first two approaches are commonly used for avalanches, especially the PCM-type or the related Voellmy-Salm type (Salm et al., 1990). Although a_0 in model (2$_1$) and (2$_2$) have similar physical interpretation, the actual value will differ. The third approach may be motivated by assuming a constant shear strength of the snowpack or flowing snow, respectively (Grigoryan, 1979). Also radar measurements may suggest a rather constant mean retarding acceleration (Gauer et al., 2007b).

5 PROBABILISTIC CALIBRATION

The probabilistic calibration of a physical model is the probabilistic solution of an inverse problem (Medina-Cetina, 2006; Yang et al., 2008). It introduces the uncertainty on available evidence (observations and physical modeling) for the integration of a joint probability distribution by the use of the Bayesian paradigm (Papoulis, 1991):

$$\pi(\mathbf{\Theta}|\mathbf{d_{obs}}) = \frac{f(\mathbf{d_{obs}}|\mathbf{\Theta}, g(\mathbf{\Theta}))\,\pi(\mathbf{\Theta})}{\int f(\mathbf{d_{obs}}|\mathbf{\Theta}, g(\mathbf{\Theta}))\,\pi(\mathbf{\Theta})\,d\mathbf{\Theta}} \tag{3}$$

where the prior $\pi(\mathbf{\Theta})$ introduces the a-priori state of information associated to the a set of parameters $\mathbf{\Theta}$, which in our case is defined as the vector of the model parameters $\mathbf{\Theta} = a_i$, where $i = 0$, $i = 0, 2$ and $i = 3$, depending on the model in use. The likelihood $f(\mathbf{d_{obs}}|\mathbf{\Theta}), g(\mathbf{\Theta})$ represents the a-priori state of information associated to the potential of the parameters $\mathbf{\Theta}$ to match the observations $\mathbf{d_{obs}}$ or to help to match them if they are embedded into the avalanche predictive model $\mathbf{g}(\mathbf{\Theta})$. The posterior $\pi(\mathbf{\Theta}|\mathbf{d_{obs}})$ is thus the joint probability function between the a-priori states of information associated to both the prior and the likelihood.

For the parameterizations of the avalanche models introduced in Equation (1), it is assumed that the coefficients a_i follow vague priors, and that the likelihood $f(\mathbf{d_{obs}}|\mathbf{\Theta})$ follows a Gaussian-type behavior.

For estimating first and second moments of the posterior, or for estimating marginal statistics for each parameter included in $\mathbf{\Theta}$, it is required to integrate the posterior with respect to the parameters. This integral can become cumbersome when the number of parameters spans in a high dimensional space. Fortunately the integral can be solved numerically. This solution yields a full description of the uncertainty associated to the model parameters $\mathbf{\Theta}$ conditioned on the available data, which contrasts typical optimization approaches (deterministic solution of inverse problems) where only one set of best estimates are retrieved.

An efficient way to solve the posterior integral is using Markov Chain Monte Carlo MCMC (Robert and Casella, 2005). A useful property of the MCMC is that it converges to the target joint density as the sample integration grows. For this work, the decision rule that determines which samples are 'accepted' or 'rejected' is the Metropolis-Hastings (MH) criteria. Under these premises, the posterior integration at the MH 'state' of the chain $s+1$ iteration is obtained by sampling a candidate point $\mathbf{Y}$ from a proposal distribution $q(.|\Theta_s)$, where the candidate point $\mathbf{Y}$ is accepted or rejected as the next step of the chain with probability given by:

$$\alpha\left(\hat{\mathbf{\Theta}}_s, \mathbf{d}_{obs}\right) = \min\left(1, \frac{\pi(\mathbf{Y}|\mathbf{d_{obs}})\,q(\hat{\mathbf{\Theta}}_s|\mathbf{Y})}{\pi(\hat{\mathbf{\Theta}}_s|\mathbf{d}_{obs})\,q(\mathbf{Y}|\hat{\mathbf{\Theta}}_s)}\right) \tag{4}$$

For the MCMC sampling, the distribution of interest $f(.|\mathbf{d_{obs}})$ appears as a ratio, so that the constant of proportionality cancels out. Additionally, the evaluation of the posterior requires discarding the first iterations called the burn-in points, before it reaches the stationary condition from which the statistical inferences are generated.

Results from the probabilistic calibration included the three proposed avalanche models: The Coulomb-

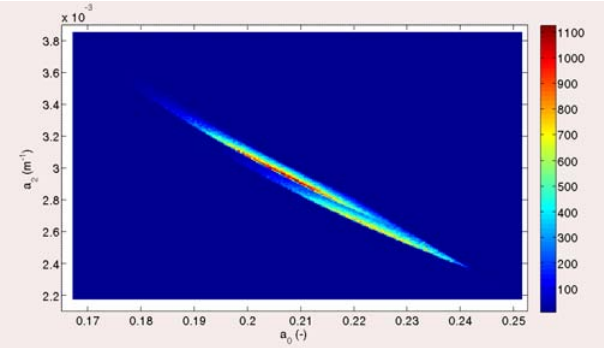

Figure 6: 2D frequency histogram of model M2 parameters.

type (M1) (2_1) , the PCM-type (M2) (2_2) and the constant deceleration-type (M3) (2_3). Information from the observations including the correlation between the velocities and run-out distance were introduced into the likelihood formulation. The priors of the model parameters were defined based on the results of previous optimization analysis performed on the same data and the same models. In this way, after the posterior integration, a full probabilistic description conditioned in the same data is retrieved for each avalanche model. For instance, Figure 6 presents the histogram of the MCMC samples obtained from M2. This figure shows

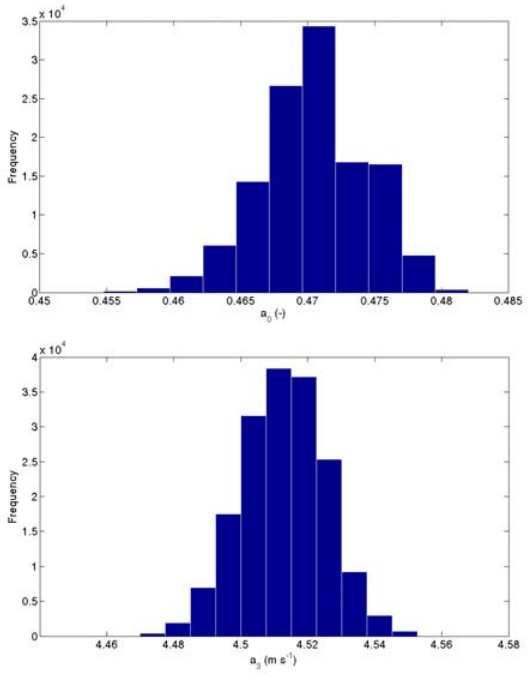

Figure 7: Frequency histogram of model parameter for M1 (top) and M3 (bottom).

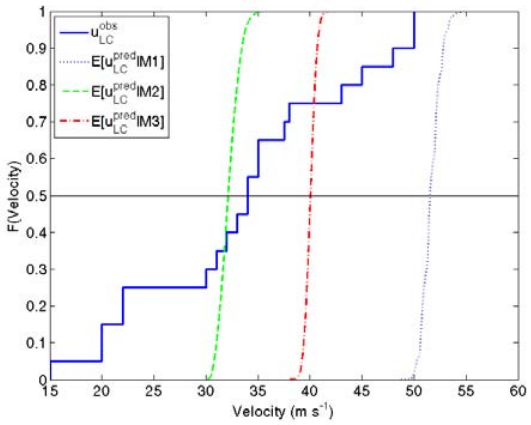

Figure 8: Comparison between expected velocity model predictions at point LC.

a bimodal distribution with non-linear relationships between parameters a_0 and a_2. These type of inferences are very appealing characteristics of the probabilistic calibration as opposed to one-best estimate of typical optimization approaches, which cannot identify associations between parameters. Figure 7 depicts the frequency histogram for the two one-parameter models M1 and M3, respectively.

The solution of the probabilistic inverse problem then can be used to simulate potential realizations of the avalanche models. These represent at each reading point (LC, CD, b, and R) the expected or average responses of each model (not the data simulation). For instance, Figure 8 shows a comparison between the cumulative density functions of the the three models of interest, representing the expected model predictions at the reading point LC. As a reference, the empirical cumulative density function of the observations is plotted in the background. From this figure is observed, that model M2 hits practically the mean of the observations, while the M1 and M3 are significantly biased. Similarly, an analysis on the run out distance (Figure 9), shows that models M1 and M2 approximate better to the mean of the observations (plotted on the background), with model M2 having the least uncertain response on the mean of the predictions. In terms of run-out distance, Model M3 performance is relatively lower compared with M1 and M2.

6 CONCLUSIONS

Simple block models are still in use for runout prediction for hazard assessment. The performance test using observed avalanche data (velocity at three points and runout distance for 22 events) shows that the two-

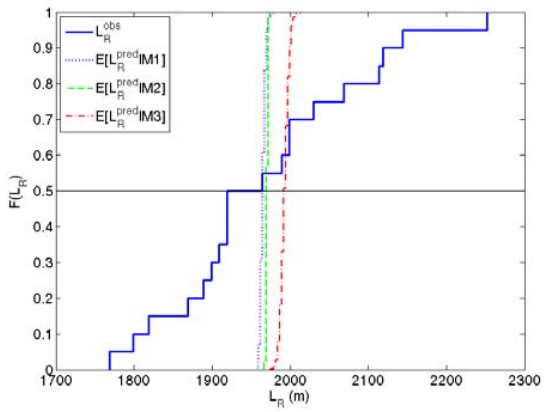

Figure 9: Comparison between expected run out model predictions.

parameter model performs best in predicating both the expected velocities and expected run out distance. This is not totally surprising; having two parameters there is more variability to tune. However, more surprising is that the constant deceleration model still preforms reasonable well. This suggests that the retarding acceleration on average seems to be rather constant during the avalanche descent, an observation that also radar measurements seem to indicate (Gauer et al., 2007b) and it is also reflected in the measured retarding accelerations (Fig. 5). On the other hand, the Coulomb-type model over-predicts the velocity at LC considerably, which suggests that the retarding acceleration in the steep part of the track is too low in this case. Taking the mean of $a_0 \, (\approx \, 0.47)$ for M1, a_{ret} is approximately -4.0 m s^{-2} compared to -4.5 m s^{-2} in the case of M3 and approximately -4.7 m s^{-2} for M2 ($a_0 = 0.2$ and $a_2 = 3 \cdot 10^{-3}$ m^{-1}) in the surrounding of LC. This implies that models based only on Coulomb frictional rheology are not able to capture the dry-snow avalanche flow.

A next aim will be to retrieve a parameter distribution that will also reflect the distribution of the observations. Although, it is not expected that the constant deceleration model M3 is cable to reproduce the low velocity tail of the observed distributions. The bowl shape topography in the upper part of the Ryggfonn path requires that the maximum a_3 is less then 4.7 m s^{-2} for model M3 to pass through the bowl. This however implies that the minimum velocity at LC will be about 30 m s^{-1}, which is on the other hand close to the observed mean. Similar limitations on the parameter choice are likely to apply also for model M2.

ACKNOWLEDGMENTS

This work was funded through NGI's SIP-program "Avalanche research". This is publication no. 210 from the International Centre for Geohazards.

REFERENCES

Ancey, C. and M. Meunier, 2004: Estimating bulk rheological properties of flowing snow avalanches from field data. *Journal of Geophysical Research*, **109**, doi:10.1029/2003JF000036.

Bakkehøi, S., U. Domaas, and K. Lied, 1983: Calculation of snow avalanche runout distance. *Annals of Glaciology*, **4**, 24–29.

Bozhinskiy, A. N., 2008: Modelling of snow avalanche dynamics: influence of model parameters. *Annals of Galciology*, **49**, 38–42.

Buser, O. and H. Frutiger, 1980: Observed maximum run-out distance of snow avalanches and the determination of the friction coefficients μ and ξ. *Journal of Glaciology*, **26**, 121–130.

Faug, T., P. Gauer, K. Lied, and M. Naaim, 2008: Overrun length of avalanches overtopping catching dams: Cross-comparison of small-scale laboratory experiments and observations from full-scale avalanches. *Journal of Geophysical Research Earth-Surfaces*, **113**, F03009, doi:10.1029/2007JF000854.

Gauer, P., D. Issler, K. Lied, K. Kristensen, H. Iwe, E. Lied, L. Rammer, and H. Schreiber, 2007a: On full-scale avalanche measurements at the Ryggfonn test site, Norway. *Cold Regions Science and Technology*, **49**, 39–53, doi:10.1016/j.coldregions.2006.09.010.

Gauer, P., M. Kern, K. Kristensen, K. Lied, L. Rammer, and H. Schreiber, 2007b: On pulsed Doppler radar measurements of avalanches and their implication to avalanche dynamics. *Cold Regions Science and Technology*, **50**, 55–71, doi:10.1016/j.coldregions.2007.03.009.

Gauer, P. and K. Kristensen, 2005: Avalanche Studies and Model Validation in Europe, SATSIE; Ryggfonn measurements: Overview and dam interaction. NGI Report 20021048-10, Norwegian Geotechnical Institute, Sognsveien 72, N-0806 Oslo.

Gauer, P., K. Lied, and K. Kristensen, 2008: On avalanche measurements at the norwegian full-scale test-site ryggfonn. *Cold Regions Science and Technology*, **51**, 138–155, doi:10.1016/j.coldregions.2007.05.005.

Grigoryan, S. S., 1979: A new law of friction and mechanism for large-scale avalanches and landslides. *Soviet Physics - Doklady*, **24**, 110–111.

Lied, K. and S. Bakkehøi, 1980: Empirical calculations of snow-avalanche run-out distance based on topographic parameters. *Journal of Galciology*, **26**, 165–177.

Medina-Cetina, Z., 2006: *Probabilistic calibration of a soil model*. Phd thesis, Johns Hopkins University, Baltimore MD, USA.

Norem, H., 1995: The Ryggfonn Project: Summary Report 1981–1995. Techreport A952-1, Dr. ing. Harald Norem A/S Consultant in Snow Engineering, Molde, Norway.

Papoulis, A., 1991: *Probability, Random Variables and Stochastic Processes*. Mc-Graw Hill, USA.

Perla, R., T. T. Cheng, and D. M. McClung, 1980: A two-parameter model of snow-avalanche motion. *Journal of Glaciology*, **26**, 119–207.

Robert, C. P. and G. Casella, 2005: *Monte Carlo Statistical Methods*. Springer, New York.

Salm, B., A. Burkard, and H. U. Gubler, 1990: Berechnung von Fliesslawinen. Eine Anleitung für Praktiker mit Beispielen. Mitt. Eidgenöss. Inst. Schnee- Lawinenforsch. 47, 37 pages, SLF, Davos, Switzerland.

Yang, S., Z. Medina-Cetina, and F. Nadim, 2008: Uncertainty analysis on remoulded undrained shear strength of marine clay. *Georisk*, submitted.